Geophysical Research Letters

RESEARCH LETTER
10.1029/2025GL117137

Role of Soil Moisture Gradients in Favoring Mesoscale Convective Systems in East China

Yutong Lu[1,2], John H. Marsham[2], Douglas J. Parker[2,3], Cornelia M. Klein[4], Christopher M. Taylor[4,5], Juan Fang[1], and Jianping Tang[1]

[1]School of Atmospheric Sciences, Nanjing Unversity, Nanjing, China, [2]Institute for Climate and Atmospheric Science, School of Earth and Environment, the University of Leeds, Leeds, UK, [3]NORCE Norwegian Research Centre AS, Bjerknes Centre for Climate Research, Bergen, Norway, [4]UK Centre for Ecology and Hydrology, Wallingford, UK, [5]National Centre for Earth Observation, Wallingford, UK

Key Points:

- Convective cores in mature mesoscale convective systems favor on drier side of sharp soil moisture (SM) gradients in East China
- SM gradients intensify surface temperature gradients, enhancing vertical wind shear and moisture convergence
- Upstream clouds reduce surface energy, amplifying effects of SM heterogeneity on storm organization

Supporting Information:

Supporting Information may be found in the online version of this article.

Correspondence to:

J. Tang,
jptang@nju.edu.cn

Citation:

Lu, Y., Marsham, J. H., Parker, D. J., Klein, C. M., Taylor, C. M., Fang, J., & Tang, J. (2025). Role of soil moisture gradients in favoring mesoscale convective systems in East China. *Geophysical Research Letters*, *52*, e2025GL117137. https://doi.org/10.1029/2025GL117137

Received 19 MAY 2025
Accepted 22 AUG 2025

Author Contributions:

Conceptualization: Yutong Lu, John H. Marsham, Jianping Tang
Data curation: Yutong Lu
Formal analysis: Yutong Lu, Cornelia M. Klein, Christopher M. Taylor
Funding acquisition: Jianping Tang
Investigation: Yutong Lu
Methodology: Yutong Lu, John H. Marsham, Cornelia M. Klein, Jianping Tang
Project administration: Juan Fang, Jianping Tang
Resources: Jianping Tang
Software: Yutong Lu, Cornelia M. Klein, Jianping Tang
Supervision: John H. Marsham, Douglas J. Parker, Jianping Tang
Validation: Cornelia M. Klein

Abstract Mesoscale convective systems (MCSs) contribute significantly to summer precipitation in the tropics and midlatitude. Although soil moisture (SM) effects on convection are globally recognized, its specific role on mature MCSs in East China remains unclear. Using convection-permitting simulations spanning 22 summers, we find that convective cores within mature MCSs preferentially develop on the drier side of strong SM gradients (~200 km). This is evidenced by a 2.5-fold increase in core occurrences downstream of the steepest 10% of SM gradients versus a near-uniform surface. SM gradients shape sensible heat flux gradients via evapotranspiration, while upstream pre-storm rain-producing clouds suppress surface available energy. These processes favor MCSs through enhancing near-surface temperature gradients which strengthen moisture convergence and zonal wind shear. Our results highlight the critical role of SM gradients in favoring MCS propagation in East China. As climate change intensifies SM heterogeneity, improved land-surface representation offers potential for advancing rainfall prediction and projection.

Plain Language Summary In summer, East China often experiences heavy rainfall from large, long-lived thunderstorm systems called mesoscale convective systems (MCSs). These storms can be influenced by how wet or dry the surface is. How soil moisture (SM) affects MCSs during their mature stage has remained uncertain. Using high-resolution regional climate simulations over 22 summers, we find that MCSs tend to intensify on the drier side of sharp SM contrasts. These dry areas heat up more quickly, creating stronger temperature contrasts near the surface. This strengthens key ingredients for sustaining strong storms including vertical wind shear and moisture convergence. We also find that earlier rain clouds upstream reduce solar radiation arriving at the surface, reinforcing this pattern. Our results show that not just how wet or dry the soil is, but how unevenly that moisture is distributed, plays a key role in storm development. As climate change increases land surface variability, improving how models represent SM and cloud–radiation interactions could enhance the prediction of severe rainfall events and their broader climate impacts.

1. Introduction

Mesoscale convective systems (MCSs) are the largest form of deep convection, consisting of organized clusters of cumulonimbus clouds and extensive upper-level cirriform clouds (Houze, 2014; Huang et al., 2018). These systems often produce severe weather hazards, including floods, hail, and tornadoes. Beyond their destructive impacts (Islam & Wang, 2024; Shi et al., 2021; J. Wang et al., 2023), MCSs play a crucial role in the global water cycle, contributing 50%–60% of annual precipitation in the deep tropics (Zhao, 2022), and 30% in mid-latitude East China (P. Li et al., 2020; Lu et al., 2025). Over land, their longevity and extended scale also make them important in redistributing energy via the vertical diabatic heating (Houze, 1989; Johnson & Ciesielski, 2000) and enhanced vertical transport.

Given their size and the mesoscale circulation they generate (Houze, 2018; Schumacher & Rasmussen, 2020), previous research on MCSs has primarily focused on large-scale atmospheric drivers of MCS development, such as moisture convergence, convective instability, and vertical wind shear (Chen et al., 2022; Feng et al., 2019; P. Li, Song, et al., 2023; Lu et al., 2024; Song et al., 2019; C. Wang et al., 2024; Q. Yang et al., 2017). However, growing evidence suggests that soil moisture (SM) can modulate convection initiation alongside the large-scale circulation forcing. Notably, even in the absence of favorable large-scale circulation conditions, a considerable number of MCSs can still form, develop and be sustained (Gaal & Iii, 2021; Song et al., 2019). Dry soil, featuring reduced

Visualization: Yutong Lu
Writing – original draft: Yutong Lu
Writing – review & editing: Yutong Lu, John H. Marsham, Douglas J. Parker, Cornelia M. Klein, Christopher M. Taylor, Juan Fang

water availability, limits evapotranspiration (Seneviratne et al., 2010) and thereby enhances sensible heat flux (SH). The resulting surface heating deepens the planetary boundary layer (PBL) and modulates the near-surface atmospheric conditions. Numerous studies, based on both models (Garcia-Carreras et al., 2011) and observations (Taylor et al., 2011), indicate that convection is more likely to occur over dry soils, particularly near regions with strong negative upwind gradients in SH. SM heterogeneity creates horizontal near-surface temperature gradients through SH, which in turn drive mesoscale circulations (Birch et al., 2013; Gaal & Iii, 2021; Taylor et al., 2011), even over complex terrain such as the Qinghai-Tibetan Plateau (Barton et al., 2021). The resulting moisture convergence, enhanced vertical wind shear, and reduced entrainment-dilution of convective boundary layer air favors deep convection, particularly in the afternoon (Garcia-Carreras et al., 2011; Taylor et al., 2007).

While SM heterogeneity is known to favor MCS initiation, recent findings indicate it might also influence the growth and propagation of mature MCSs. Observational evidence in West Africa reveals that dry soils can enhance convective inhibition, weakening convections (Taylor et al., 2010). Additional modeling studies further support this feedback (Gantner & Kalthoff, 2010). On the other hand, (Klein & Taylor, 2020) showed that dry soil anomalies of ∼200 km in scale can strengthen climatological temperature gradients in the semi-arid Sahel. Their findings suggest that pre-storm dry soil patches, which heat and deepen the PBL, can further enhance convection and promote the maturation of MCSs. Building on these findings from the Sahel, an ideal natural laboratory for MCS-SM interactions, Barton et al. (2025) extended the analysis to a global scale. They demonstrated that mesoscale SM gradients can enhance MCSs across multiple continents by strengthening vertical wind shear. Extending beyond its sub-daily- to daily-scale influence, springtime SM exerts delayed seasonal influence, promoting nocturnal growth of summer MCSs over the U.S. Great Plains (Hu et al., 2021).

Despite the growing evidence of the role of SM controls on MCSs, the influence of SM on propagating convection in East China remains largely unexplored. East China is a hotspot for MCS activity during the warm season due to strong moisture convergence associated with the East Asian summer monsoon (EASM) and vertical wind shear provided by the mid-level East Asian westerly jet. MCSs in East China typically exhibit an south-eastward propagation pattern consistent with prevailing large-scale flow patterns (Guo et al., 2022; Lu et al., 2024; R. Yang et al., 2019). Given the persisting nature of SM, previous studies on SM-precipitation coupling in East China have mainly focused on non-local effects associated with unorganized convection on longer timescales (Gao et al., 2020; Meng et al., 2014; Zhan & Lin, 2011; Zuo & Zhang, 2016). Fewer studies have explored its mesoscale effect on precipitation (Z. Li et al., 2015; J. Zhang et al., 2011; Zhong et al., 2018). Observational study suggested that local precipitation largely depends on the pre-storm atmospheric environment (J. Zhang et al., 2022), with a tendency for afternoon precipitation in North China to occur over dry soil (S. Li et al., 2024). These findings highlight the role of pre-storm SM and atmospheric conditions in initiating subsequent consecutive convective precipitation. However, their impact on growth and propagation of organized deep convection in East China remains unexamined.

In a warming future, the increasing frequency of abrupt dry-wet alternation is expected to amplify SM heterogeneity over East China (Qiu et al., 2024). This projected intensification underscores the urgency of understanding how SM modulates MCS development. Building on previous observational work by Klein and Taylor (2020) on pre-storm SM effects on convective cores within mature MCSs in the Sahel, this study explores its role in East China based on convection-permitting (CP) scale Weather Research and Forecasting (WRF) model outputs.

2. Data and Methods

2.1. Data

This study examines the relationship between mature MCSs and SM in East China using long-term (2000–2021) convection-permitting (CP) regional climate simulations with the WRF model, v4.3.3 (Skamarock et al., 2019). ERA5 reanalysis (Hersbach et al., 2020) provided boundary and initial conditions. The model domain covers East China at 4 km resolution on an 840 × 840 grid under Lambert projection (Figure S1 in Supporting Information S1), with 50 vertical levels extending to 50 hPa and a 15-layer sponge boundary. Simulations span 23 summers (1999–2021), each initialized on 21 May and integrated until 1 September, using a 10-day spin-up. Key physical parameterizations included the WRF single-moment (WSM5) scheme (Hong et al., 2004) for microphysics, Yonsei University (YSU) Scheme (Hong et al., 2006) for PBL processes, the Community Atmosphere Model schemes (Collins et al., 2004) for shortwave and longwave radiation, and the Noah-MP land surface model

(Niu et al., 2011). The cumulus convective parameterization was switched off to explicitly resolve convection. The simulation is hereafter referred to as WRF-CPM. WRF-CPM reproduces MCS climatology and rainfall but overestimates extremes (Lu et al., 2025). It also captures MCS precipitation responses to zonal wind shear and total column water vapor (TCWV). WRF-CPM also realistically simulates the interactions among SM, precipitation, and convection (Figures S2 and S3 in Supporting Information S1).

2.2. Methods

Cloud top temperature (Tb) from the WRF-CPM simulations was estimated using the Community Radiative Transfer Model (Weng et al., 2005) simulating the Himawari-8 11.2 μm channel. WRF-CPM inputs included pressure, temperature, water vapor, and the mass mixing ratio of cloud water, rainwater, graupel, snow ice, along with surface temperature. SM, near-surface variables, and energy fluxes–sensible heat (SH) and latent heat (LH)–were also extracted. Available energy (AE) was calculated as the sum of SH and LH, and the evaporative fraction (EF) was defined as the ratio of LH/(SH + LH).

Convective cores were defined as regions with extensive cloud coverage (Tb ≤ -40°C) spanning at least 15,000 km^2 for every full hour. These cores, characterized by intense rainfall and direct PBL connection through deep updrafts, were distinguished from surrounding stratiform cloud shields. Following Klein et al. (2018), a two-dimensional wavelet scale decomposition was applied to the Tb field. Core centers were determined as local power maxima within 30 × 30 km^2 windows at scales of 24–90 km. Only cores embedded in MCSs identified from WRF-CPM were retained. To ensure a sample of mature, propagating MCSs, cores associated with MCSs initiated within 100 km were excluded. The analysis was conducted at 1700 BJT, which corresponds to the diurnal peak of mature MCS activity in eastern China (Figure S4 in Supporting Information S1). The mature stage was defined as the time when MCSs exhibited maximum convective area accompanied by stratiform regions (Roca et al., 2017). To minimize the influence of pre-storm rainfall on SM, cores with rainfall before 1100 BJT on the storm day were excluded. These filtering criteria yielded 361 cores of 9,348 cores at 1700 BJT, the typical MCS maturation peak in East China (excluding the east Tibetan Plateau). Among these, 57.81% exhibited southward propagation (Data and Methods, and Figure S1 in Supporting Information S1).

Anomalies were calculated for each pixel and time of day relative to the 2000–2021 JJA climatology. We focused on anomalies at 1100 BJT on storm days to capture established surface ahead of mature storm development. Gradients were computed using a finite differencing approach along the meridional direction as the difference between adjacent latitudinal grid points. A perturbation test with bootsrapping framework (Gaal & Iii, 2021) was applied to assess the significance of pre-storm land conditions, accounting for both temporal and spatial correlations in the SM fields. SM composites were randomly sampled from different years, repeated 1,000 times to build an empirical distribution. Pixels exceeding two-tailed quantile thresholds were considered significant.

To assess how solar radiation and SM evaporation modulate near-surface atmosphere, multiple linear regression (MLR) was employed. MLR estimates linear relationships between a response variable and multiple predictors using the least squares method.

For two independent variables, the MLR equation is be expressed as:

$$\boldsymbol{Y = \alpha_1 x_1 + \alpha_2 x_2 + \beta + \varepsilon}$$

Here, $\boldsymbol{\alpha_1}$ and $\boldsymbol{\alpha_2}$ are slope coefficients, $\boldsymbol{\beta}$ is the intercept (constant term), and $\boldsymbol{\varepsilon}$ represents the residuals. In this study, $\boldsymbol{Y}$ denotes SH anomalies, $\boldsymbol{x}_1$ represents AE anomalies, and $\boldsymbol{x_2}$ corresponds to EF anomalies. The predicted values of $\boldsymbol{Y}$ are represented as:

$$\boldsymbol{Y' = \alpha_1 x_1 + \alpha_2 x_2 + \beta}$$

The variation explained by the predicted values could be expressed by:

$$\boldsymbol{PE = \frac{SSY'}{SSY}},$$

where:

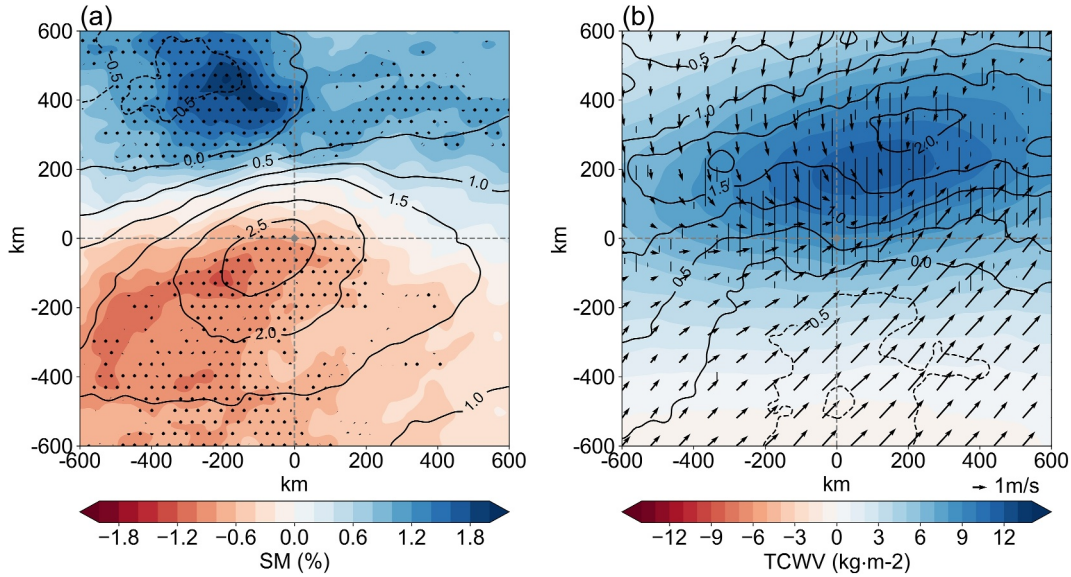

Figure 1. *Pre-storm (1100 BJT) surface and low-level atmospheric conditions*. (a, b) Composites centered on 1700 BJT convection cores within mesoscale convective systems. (a) Anomalous soil moisture (SM) (shading, unit: %, percentage of volumetric soil moisture) and 2 m potential temperature (θ; black contour, unit: K). (b) Anomalous total column water vapor (shading, unit: kg/m^2), 10 m AGL wind (vectors), 3,000–50 m zonal wind shear (black contours, unit: m/s), and regions with 50 m AGL convergence ($\leq -5 \times 10^{-6}$ s^{-1}, hatched). Dots in panel (a) indicate significant anomalies of SM at the 99% level.

$$SSY = \sum_{i=1}^{i=n} (Y_i - \overline{Y})^2, SSY' = \sum_{i=1}^{i=n} (Y_i' - \overline{Y'})^2,$$

$\overline{Y}$ and $\overline{Y'}$ denote the mean values for Y and Y'.

To partition contributions of two correlated predictors, full regression model with reduced models excluding one predictor at a time were compared. The unique sum of squares (SS) was calculated as the difference between full and reduced model SS. The compound SS, representing the shared variance between predictors, was obtained by subtracting the sum of unique SS values from the total SS. This quantifies individual and shared contributions of correlated predictors.

Given the non-simultaneous effects of radiation and energy, cumulative energy from 0800 to 1100 BJT was used in the MLR analysis. Extreme EF values resulting from low AE were filtered by retaining EF values with absolute values $\leq$10 and accumulated AE $\geq$ 200 W/m^2.

3. Results

3.1. Pre-Storm Surface and Atmosphere Conditions

Figure 1 illustrates the relationship between the anomalous soil moisture (SMA) and low-level atmospheric conditions at 1100 BJT. Late-afternoon convective cores to occur over dry soil and a warm PBL, where a pronounced south-north SMA gradient extends approximately 200 km northward. This region also exhibits a steep north-south gradient in 2 m potential temperature (θ, Figure 1a), with wet soil and cooler near-surface atmosphere to the north and dry soil with warm near-surface air to the south (Figure 1a).

Additionally, these convective cores preferentially develop near regions of enhanced zonal wind shear (Figure 1b), which aligns with the 2 m θ gradient. Anomalous convergence is evident over this gradient, forming a distinct southwest-to-northeast-tilted band north of the convective cores (Figure 1b). Moreover, late-afternoon cores are often centered within an anomalously moist PBL (TCWV anomaly $\sim$ 12 kg/m^2) which coincides with near-surface convergence (Figure 1b). This convergence is further supported by enhanced southerly winds to the south and northerly winds to the north, creating a cyclonic anomaly above the moisture anomaly (Figure 1b).

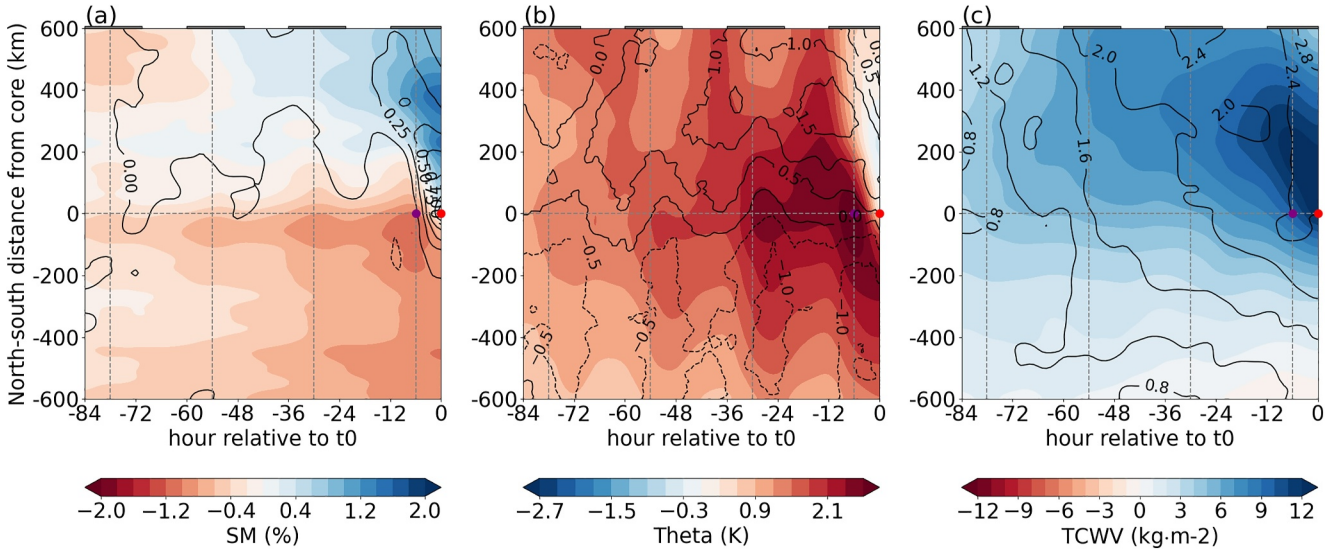

Figure 2. *Evolution of surface and atmosphere conditions and precipitation until storm time*. (a–c) Composite anomalous surface, atmosphere, and precipitation fields in the 84 hr preceding mature convective cores at 1700 BJT (t_0), shown as a function of north-south distance. (a) Anomalous soil moisture (shading, unit: %, percentage of volumetric soil moisture) and precipitation (contours, unit: mm/hr). (b) 2 m potential temperature (θ; contours, unit: K) and 3,000–50 m zonal wind shear (contours, unit: m/s), (c) Anomalous total column water vapor (shading, unit: kg/m^2) and 50 m equivalent potential temperature (θ_e; contours, units: K). Gray bars indicate daytime, the red dot indicates storm time (1700 BJT) and purple dot indicates 1100 BJT.

The combined effects of wind shear, increased PBL humidity, and near-surface convergence create favorable conditions for intense, organized convection.

We further considered the frequency distribution of along-wind SMA gradient upstream of convective cores (Figure S4a in Supporting Information S1) and compared it with a baseline distribution obtained from random sampling in the region. The distribution of SMA gradient associated with 1700 BJT convective core sample exhibits a leftward shift relative to the control sample (Figure S4a in Supporting Information S1), indicating a preference for stronger negative gradients. To quantify this relationship, we identified SMA gradient intervals corresponding to the first decile (0%–10%, strongest) and central decile (45%–55%, moderate) of the control distribution. Notably, 16% of convective cores occurred within the first decile (<−5.5%/100 km), which is 2.5 times more frequent than their occurrence within the central decile. This suggests that mature convection cores are 2.5 times more likely to develop under strong SMA gradients compared to near-uniform surface conditions. Moreover, the frequency of convective core occurrence within the strongest gradient range increased by 63% relative to the control distribution.

We now examine how dry soil and SMA gradients influence atmospheric conditions leading to intense convection. Figure 2 depicts the anomalous evolution of surface and atmospheric fields during the 84 hr preceding convective cores within mature MCSs.

Throughout the 3 days leading up to the event, SM remains anomalously dry (∼−0.8%) at late-afternoon core locations (Figure 2a). Meanwhile, wet SMA emerges ∼400 km north of these core locations, gradually intensifying and expanding southward. By the day of the storm, these wet anomalies extend to ∼200 km north of the cores (Figure 2a). As drier conditions persist to the south, a pronounced SMA gradient develops, becoming evident approximately 54 hr before the storm (Figure 2a).

The warm PBL anomaly seen in Figure 1 begins forming during previous daytime periods when dry SMA is already well established. A strong near-surface θ gradient rapidly develops after sunrise on the day of the storm (Figure 2b). Concurrently, zonal wind shear (Figure 2b) exhibits a southward propagation trend in response to diurnal θ variations starting 3 days before the storm. By sunrise on the storm day, an enhanced zonal wind shear (∼1.6 m/s) is evident, coinciding with the intensifying 2 m θ gradient.

Additionally, anomalous TCWV has been present for at least 5 days before storm time (not shown), strengthening north of the core locations from 3 days prior (Figure 2c). A distinct southward propagation of TCWV anomalies

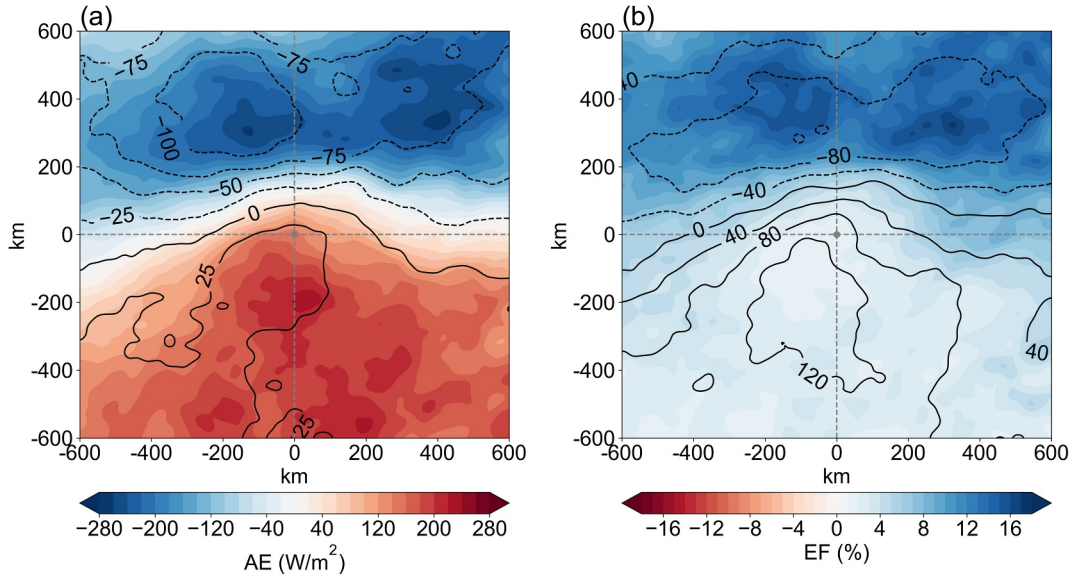

Figure 3. *Surface energy conditions preceding mesoscale convective systems* (*MCSs*). Composites centered on 1700 BJT convective cores within MCSs, showing anomalous (a) available energy (AE; shading, unit: W/m^2) and sensible heat flux (SH; contours, unit: W/m^2), and (b) evaporative fraction (EF; shading, units: %) and latent heat flux (LH; contours, units: W/m^2) based on accumulated fluxes between 0800 and 1100 BJT.

becomes apparent approximately 18 hr ahead of the storm (Figure 2c). This evolution is also evident in equivalent potential temperature (θ_e) anomalies at 50 m AGL, which reflect the combined influence of moisture and temperature on atmospheric instability (Figure 2c). Throughout the pre-storm period, θ_e anomalies gradually intensify. After sunrise, θ_e anomalies rapidly intensify southward, following the sharp increase in near-surface θ anomalies and the rapid establishment of a strong θ anomaly gradient.

To understand how the SMA gradient develops, we examine the evolution of precipitation 84 hr leading up to the storm. There are positive rainfall anomalies to the north and sustained negative anomalies to the south during the daytime, approximately 78 hr before the storms (Figure 2a). Starting from the night before the day of the storm, northern precipitation anomaly exhibits a clear southward propagation trend. This persistent precipitation in the north alters the spatial distribution of SM, gradually strengthening the SMA gradient.

3.2. Pre-Storm Surface Energy Conditions

The rapid development of an anomalous near-surface θ gradient alongside SMA gradient as shown in Figure 2, suggests that SM heterogeneity plays a key role in modulating the near-surface atmosphere. Therefore, we conclude that SM variations contribute to the formation of an anomalous near-surface temperature gradient before MCS arrival, through their influence on sensible energy partitioning. To evaluate this effect, we now examine the pre-storm surface energy fluxes.

Sensible heat flux (SH) anomalies exhibit a spatial pattern broadly consistent with SMA (Figure 3a), with enhanced surface heating over the drier south and suppressed heating to the wetter north. However, unlike the Sahel—where SH, SM, and PBL temperature anomalies are tightly coupled preceding mature MCSs—the spatial and temporal correspondence between SH, SM, and 2 m temperature anomalies in East China is weaker (Figure 3a and Figure S6c in Supporting Information S1). Latent heat flux (LH) anomalies show a similar south-north contrast, with enhanced LH over the drier soil (Figure 3b). Taken together, these signals point to an additional control on the surface-energy budget, likely the radiative impact of pre-storm cloud cover, whose role we assess below.

A further analysis of cloud cover effects reveals a strong south-north contrast in AE centered around the core locations (Figure 3a). To the north, a pronounced reduction of AE associated with extensive cloud coverage indicates limited surface energy available for heating the near-surface atmosphere, thereby reinforcing the strong

temperature gradient. This cooling is linked to preceding precipitation, as shown in Figure 2a, where rain-producing clouds reduce solar radiation. This is further evidenced by the temporal evolution of downward shortwave radiation (DSR). The reduced DSR evolves with daytime pre-storm precipitation with suppressed center occur 3 days ahead and peaks at noon on storm day (Figure S6a in Supporting Information S1), modulating SH (Figure S6a in Supporting Information S1), and LH evolution (Figure S6b in Supporting Information S1). SM modulates the PBL by regulating evaporation, which affects both moisture content and the balance between LH and SH, ultimately controlling PBL temperature and depth. The anomalous EF distribution shows a strong correlation with both SMA and PBL θ anomaly (Figure 3b and Figure S6d in Supporting Information S1). To quantify the contributions of cloud effect and SM to pre-storm PBL modulation, we conducted a MLR analysis on SH anomalies against AE and EF anomalies. Since surface flux effects on the PBL are cumulative, SH and EF were accumulated over 0800–1100 BJT. The MLR results indicate that EF anomalies account for 27% of SH variability, while AE anomalies contribute 17%, with their combined effect explaining 40% of the variability.

The analysis indicates that both SMA and cloud cover heterogeneity caused by preceding rainfall play a role in modulating the PBL before mature MCS development, with SM having a stronger influence. These factors enhance the meridional temperature gradient, which in turn strengthens zonal wind shear along the temperature gradient.

The PBL remains anomalously moist for at least 5 days before the storm and experiences additional moistening overnight prior to MCS development. Near-surface convergence, driven by enhanced PBL warming over and to the south of the core location, further contributes to moisture convergence. The impact of preceding diurnal variation in rainfall is particularly notable, as it influences both the SMA gradient and the reduction of AE due to rain cloud cover in the north.

4. Conclusions

Figure 4 schematically illustrates the atmospheric feedback mechanisms underlying the preference of convective cores embedded in mature MCSs in East China. These mechanisms broadly align with those identified in the Sahel, and this study extends and refines the framework of Klein and Taylor (2020) to the East Asia context. The convection-permitting model simulation shows a robust tendency for afternoon MCS cores to develop along the southern, drier boundary of the SMA gradient. Pre-storm northern rainfall induces SMA gradients, causing spatial SH and LH contrasts via differential surface evaporation. Drier soils enhance SH and rapidly warm the near-surface air, while wetter soils increase latent cooling. The resulting near-surface θ anomaly gradients enhance zonal wind shear and low-level convergence, favoring MCS propagation.

The presence of dry soil, persisting for at least 5 days (not shown) and intensifying 3 days before the storm, plays a crucial role in triggering low-level convergence and facilitating overnight moisture accumulation. Additionally, pre-storm cloud cover over wetter regions reduces incoming solar radiation, further altering the AE distribution and amplifying near-surface temperature contrasts. Although the intensity of the EASM modulates the SMA magnitude and influences moisture sources (Figure S8 in Supporting Information S1), the underlying mechanism identified remains robust.

Similar to the Sahel, antecedent rainfall in East China contributes to the establishment of a large-scale (~200 km, Figure S5 in Supporting Information S1) SMA gradient 3 days prior to the MCS event. However, the geometric SM pattern differs markedly. In the Sahel, dry soil patches are nearly centered on the upwind of the convection and display near-meridional symmetry (Klein & Taylor, 2020). In contrast, East China dry soil patches feature a strong meridional dry-wet transition, with convection cores preferentially developing downwind of sharp meridional SMA gradients.

This study underscores the critical role of SM in modulating MCS development in East China through a combination of dynamic and thermodynamic processes, as revealed by convection-permitting model simulations. While the simulated MCSs may not perfectly replicate real-world systems, the model could capture key dynamic responses (P. Li, Muetzelfeldt, et al., 2023), such as shear effects (Maybee et al., 2024) and land-atmosphere interactions (Dai et al., 2021; L. N. Zhang et al., 2023) associated with convection, allowing for meaningful quantification. Our findings highlight key differences in how mature MCSs are triggered and sustained between mid-latitudes (East China) and tropics (West Africa). In East China, preceding rainfall plays an essential role by

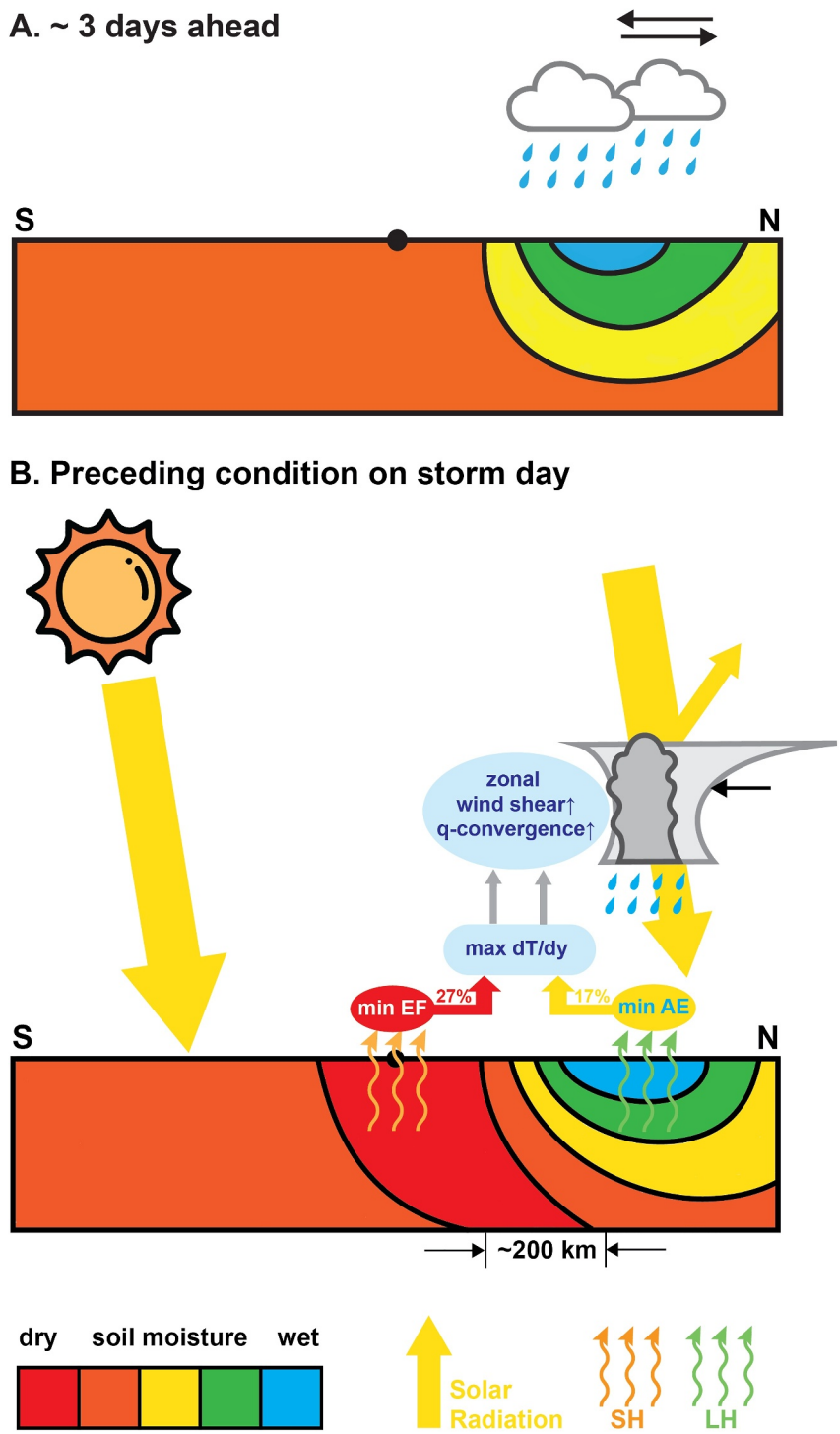

Figure 4. *Schematic diagram of soil moisture* (*SM*) *gradient influencing mesoscale convective system* (*MCS*) *intensity.* (a) Approximately 3 days before MCS development, non-MCS daytime rainfall occurs north of the core locations, moistens the northern soil, gradually establishing an SM anomaly gradient. (b) On the storm day, the SM gradient reaches its peak, with a length scale of ~200 km. Both MCS cloud cover, which reduces available energy, and the anomalous soil moisture gradient contribute to the variations in evaporative fraction, thereby modulating near-surface temperature. Their respective contributions are 17% and 27%, resulting in maximum near-surface temperature anomaly gradients, which enhance zonal wind shear and increase moisture convergence.

modulating both SM and radiation, which in turn shape the atmospheric conditions favorable for MCS development. Within East China, this study opens a new opportunity for predicting MCS rainfall based on SM patterns, which could be integrated into the training of deep-learning models.

Under global warming, SM heterogeneity is projected to enhance (Zhu et al., 2020). Observations have already indicated increased frequency of drought-pluvial transitions (Qing et al., 2023), and longer dry spells (X. Wang et al., 2022). Such amplified SM contrasts may promote more organized MCSs through the land-PBL-convection interaction mechanism in the future (Barton et al., 2025).

Data Availability Statement

Code and data generating analysis and plots for this research are available publicly at Lu (2025).

Acknowledgments
This work was funded by the National Natural Science Foundation of China (U2242204). J.H.M., D.J.P., C.M.K, and C.M.T acknowledge funding from project LMCS by NERC (NE/W001888/1). The authors would also like to thank Dr Ben Maybee, Dr Emma Barton, and Dr Weicheng Liu for related discussion and helpful comments on the study.

References

Barton, E. J., Klein, C., Taylor, C. M., Marsham, J., Parker, D. J., Maybee, B., et al. (2025). Soil moisture gradients strengthen mesoscale convective systems by increasing wind shear. *Nature Geoscience*, *18*(4), 1–7. https://doi.org/10.1038/s41561-025-01666-8

Barton, E. J., Taylor, C. M., Klein, C., Harris, P. P., & Meng, X. (2021). Observed soil moisture impact on strong convection over mountainous Tibetan Plateau. *Journal of Hydrometeorology*, *22*(3), 561–572. https://doi.org/10.1175/JHM-D-20-0129.1

Birch, C. E., Parker, D. J., O'Leary, A., Marsham, J. H., Taylor, C. M., Harris, P. P., & Lister, G. M. S. (2013). Impact of soil moisture and convectively generated waves on the initiation of a West African mesoscale convective system. *Quarterly Journal of the Royal Meteorological Society*, *139*(676), 1712–1730. https://doi.org/10.1002/qj.2062

Chen, Y., Luo, Y., & Liu, B. (2022). General features and synoptic-scale environments of mesoscale convective systems over South China during the 2013–2017 pre-summer rainy seasons. *Atmospheric Research*, *266*, 105954. https://doi.org/10.1016/j.atmosres.2021.105954

Collins, W., Rasch, P., Boville, B., Hack, J., Mccaa, J., Williamson, D., & Kiehl, J. (2004). Description of the NCAR community atmosphere model (CAM 3.0). *NCAR Technical Note, TN-464+STR*.

Dai, Y., Williams, I. N., & Qiu, S. (2021). Simulating the effects of surface energy partitioning on convective organization: Case study and observations in the US southern great plains. *Journal of Geophysical Research: Atmospheres*, *126*(2), e2020JD033821. https://doi.org/10.1029/2020JD033821

Feng, Z., Houze, R. A., Leung, L. R., Song, F., Hardin, J. C., Wang, J., et al. (2019). Spatiotemporal characteristics and large-scale environments of mesoscale convective systems east of the Rocky Mountains. *Journal of Climate*, *32*(21), 7303–7328. https://doi.org/10.1175/JCLI-D-19-0137.1

Gaal, R., & Iii, J. L. K. (2021). Soil moisture influence on the incidence of summer mesoscale convective systems in the U.S. Great Plains. *Monthly Weather Review*, *149*(12), 3981–3994. https://doi.org/10.1175/MWR-D-21-0140.1

Gantner, L., & Kalthoff, N. (2010). Sensitivity of a modelled life cycle of a mesoscale convective system to soil conditions over West Africa. *Quarterly Journal of the Royal Meteorological Society*, *136*(S1), 471–482. https://doi.org/10.1002/qj.425

Gao, C., Li, G., Xu, B., & Li, X. (2020). Effect of spring soil moisture over the Indo-China Peninsula on the following summer extreme precipitation events over the Yangtze River basin. *Climate Dynamics*, *54*(9), 3845–3861. https://doi.org/10.1007/s00382-020-05187-5

Garcia-Carreras, L., Parker, D. J., & Marsham, J. H. (2011). What is the mechanism for the modification of convective cloud distributions by land surface–induced flows? *Journal of the Atmospheric Sciences*, *68*(3), 619–634. https://doi.org/10.1175/2010JAS3604.1

Guo, Z., Tang, J., Tang, J., Wang, S., Yang, Y., Luo, W., & Fang, J. (2022). Object-based evaluation of precipitation systems in convection-permitting regional climate simulation over eastern China. *Journal of Geophysical Research: Atmospheres*, *127*(1), e2021JD035645. https://doi.org/10.1029/2021JD035645

Hersbach, H., Bell, B., Berrisford, P., Hirahara, S., Horányi, A., Muñoz-Sabater, J., et al. (2020). The ERA5 global reanalysis. *Quarterly Journal of the Royal Meteorological Society*, *146*(730), 1999–2049. https://doi.org/10.1002/qj.3803

Hong, S.-Y., Dudhia, J., & Chen, S.-H. (2004). A revised approach to ice microphysical processes for the bulk parameterization of clouds and precipitation. *Monthly Weather Review*, *132*(1), 103–120. https://doi.org/10.1175/1520-0493(2004)132<0103:ARATIM>2.0.CO;2

Hong, S.-Y., Noh, Y., & Dudhia, J. (2006). A new vertical diffusion package with an explicit treatment of entrainment processes. *Monthly Weather Review*, *134*(9), 2318–2341. https://doi.org/10.1175/MWR3199.1

Houze, R. A., Jr. (1989). Observed structure of mesoscale convective systems and implications for large-scale heating. *Quarterly Journal of the Royal Meteorological Society*, *115*(487), 425–461. https://doi.org/10.1002/qj.49711548702

Houze, R. A., Jr. (2014). *Cloud dynamics*. Academic Press.

Houze, R. A., Jr. (2018). 100 Years of research on mesoscale convective systems. *Meteorological Monographs*, *59*(1), 17.1–17.54. https://doi.org/10.1175/AMSMONOGRAPHS-D-18-0001.1

Hu, H., Leung, L. R., & Feng, Z. (2021). Early warm-season mesoscale convective systems dominate soil moisture–precipitation feedback for summer rainfall in central United States. *Proceedings of the National Academy of Sciences of the United States of America*, *118*(43), e2105260118. https://doi.org/10.1073/pnas.2105260118

Huang, X., Hu, C., Huang, X., Chu, Y., Tseng, Y., Zhang, G. J., & Lin, Y. (2018). A long-term tropical mesoscale convective systems dataset based on a novel objective automatic tracking algorithm. *Climate Dynamics*, *51*(7), 3145–3159. https://doi.org/10.1007/s00382-018-4071-0

Islam, M. Z., & Wang, C. (2024). Cost of high-level flooding as a consequence of climate change driver? A case study of China's flood-prone regions. *Ecological Indicators*, *160*, 111944. https://doi.org/10.1016/j.ecolind.2024.111944

Johnson, R. H., & Ciesielski, P. E. (2000). Rainfall and radiative heating rates from TOGA COARE atmospheric budgets. *Journal of the Atmospheric Sciences*, *57*(10), 1497–1514. https://doi.org/10.1175/1520-0469(2000)057<1497:RARHRF>2.0.CO;2

Klein, C., Belušić, D., & Taylor, C. M. (2018). Wavelet scale analysis of mesoscale convective systems for detecting deep convection from infrared imagery. *Journal of Geophysical Research: Atmospheres*, *123*(6), 3035–3050. https://doi.org/10.1002/2017JD027432

Klein, C., & Taylor, C. M. (2020). Dry soils can intensify mesoscale convective systems. *Proceedings of the National Academy of Sciences of the United States of America*, *117*(35), 21132–21137. https://doi.org/10.1073/pnas.2007998117

Li, P., Moseley, C., Prein, A. F., Chen, H., Li, J., Furtado, K., & Zhou, T. (2020). Mesoscale convective system precipitation characteristics over East Asia. Part I: Regional differences and seasonal variations. *Journal of Climate*, *33*(21), 9271–9286. https://doi.org/10.1175/JCLI-D-20-0072.1

Li, P., Muetzelfeldt, M., Schiemann, R., Chen, H., Li, J., Furtado, K., & Zhuang, M. (2023). Sensitivity of simulated mesoscale convective systems over East Asia to the treatment of convection in a high-resolution GCM. *Climate Dynamics*, *60*(9), 2783–2801. https://doi.org/10.1007/s00382-022-06471-2

Li, P., Song, F., Chen, H., Li, J., Prein, A. F., Zhang, W., et al. (2023). Intensification of mesoscale convective systems in the East Asian rainband over the past two decades. *Geophysical Research Letters*, *50*(16), e2023GL103595. https://doi.org/10.1029/2023GL103595

Li, S., Guo, J., Zhang, X., Tong, B., Su, T., Wei, J., & Li, Z. (2024). Preference of afternoon precipitation over dry soil in the north China plain during warm seasons. *Journal of Geophysical Research: Atmospheres*, *129*(8), e2023JD040641. https://doi.org/10.1029/2023JD040641

Li, Z., Zhou, T., Chen, H., Ni, D., & Zhang, R.-H. (2015). Modelling the effect of soil moisture variability on summer precipitation variability over East Asia. *International Journal of Climatology*, *35*(6), 879–887. https://doi.org/10.1002/joc.4023

Lu, Y. (2025). Role of soil moisture gradients in favouring mesoscale convective systems in East China [Dataset]. *Zenodo*. https://doi.org/10.5281/zenodo.15303525

Lu, Y., Marsham, J. H., Tang, J., Parker, D. J., & Fang, J. (2025). Summer mesoscale convective systems in convection-permitting simulation using WRF over East China. *Journal of Geophysical Research: Atmospheres*, *130*(8), e2025JD043653. https://doi.org/10.1029/2025JD043653

Lu, Y., Tang, J., Xu, X., Tang, Y., & Fang, J. (2024). Characteristics of warm-season mesoscale convective systems over the Yangtze–Huaihe river basin (YHR): Comparison between radar and satellite. *Journal of Geophysical Research: Atmospheres*, *129*(1), e2023JD038924. https://doi.org/10.1029/2023JD038924

Maybee, B., Marsham, J. H., Klein, C. M., Parker, D. J., Barton, E. J., Taylor, C. M., et al. (2024). Wind shear effects in convection–permitting models influence MCS rainfall and forcing of tropical circulation. *Geophysical Research Letters*, *51*(17), e2024GL110119. https://doi.org/10.1029/2024GL110119

Meng, L., Long, D., Quiring, S. M., & Shen, Y. (2014). Statistical analysis of the relationship between spring soil moisture and summer precipitation in East China. *International Journal of Climatology*, *34*(5), 1511–1523. https://doi.org/10.1002/joc.3780

Niu, G.-Y., Yang, Z.-L., Mitchell, K. E., Chen, F., Ek, M. B., Barlage, M., et al. (2011). The community Noah land surface model with multiparameterization options (Noah-MP): 1. Model description and evaluation with local-scale measurements. *Journal of Geophysical Research*, *116*(D12), D12109. https://doi.org/10.1029/2010JD015139

Qing, Y., Wang, S., Yang, Z.-L., & Gentine, P. (2023). Soil moisture−atmosphere feedbacks have triggered the shifts from drought to pluvial conditions since 1980. *Communications Earth & Environment*, *4*(1), 254. https://doi.org/10.1038/s43247-023-00922-2

Qiu, J., He, C., Liu, X., Gao, L., Tan, C., Wang, X., et al. (2024). Projecting dry-wet abrupt alternation across China from the perspective of soil moisture. *Npj Climate and Atmospheric Science*, *7*(1), 1–13. https://doi.org/10.1038/s41612-024-00808-w

Roca, R., Fiolleau, T., & Bouniol, D. (2017). A simple model of the life cycle of mesoscale convective systems cloud shield in the tropics. https://doi.org/10.1175/JCLI-D-16-0556.1

Schumacher, R. S., & Rasmussen, K. L. (2020). The formation, character and changing nature of mesoscale convective systems. *Nature Reviews Earth & Environment*, *1*(6), 300–314. https://doi.org/10.1038/s43017-020-0057-7

Seneviratne, S. I., Corti, T., Davin, E. L., Hirschi, M., Jaeger, E. B., Lehner, I., et al. (2010). Investigating soil moisture–climate interactions in a changing climate: A review. *Earth-Science Reviews*, *99*(3), 125–161. https://doi.org/10.1016/j.earscirev.2010.02.004

Shi, W., Li, X., Zeng, M., Zhang, B., Wang, H., Zhu, K., & Zhuge, X. (2021). Multi-model comparison and high-resolution regional model forecast analysis for the "7.20" Zhengzhou severe heavy rain. *Transactions of Atmospheric Sciences*, *44*(5), 688–702. https://doi.org/10.13878/j.cnki.dqkxxb.20210823001

Skamarock, W. C., Klemp, J. B., Dudhia, J., Gill, D. O., Barker, D. M., Duda, M. G., et al. (2019). A description of the advanced research WRF version 4. *NCAR Tech. Note Ncar/Tn-556+ Str, 145*.

Song, F., Feng, Z., Leung, L. R., Houze, R. A., Jr., Wang, J., Hardin, J., & Homeyer, C. R. (2019). Contrasting spring and summer large-scale environments associated with mesoscale convective systems over the U.S. Great Plains. *Journal of Climate*, *32*(20), 6749–6767. https://doi.org/10.1175/JCLI-D-18-0839.1

Taylor, C. M., Gounou, A., Guichard, F., Harris, P. P., Ellis, R. J., Couvreux, F., & De Kauwe, M. (2011). Frequency of Sahelian storm initiation enhanced over mesoscale soil-moisture patterns. *Nature Geoscience*, *4*(7), 430–433. https://doi.org/10.1038/ngeo1173

Taylor, C. M., Harris, P. P., & Parker, D. J. (2010). Impact of soil moisture on the development of a Sahelian mesoscale convective system: A case-study from the AMMA special observing period. *Quarterly Journal of the Royal Meteorological Society*, *136*(S1), 456–470. https://doi.org/10.1002/qj.465

Taylor, C. M., Parker, D. J., & Harris, P. P. (2007). An observational case study of mesoscale atmospheric circulations induced by soil moisture. *Geophysical Research Letters*, *34*(15), L15801. https://doi.org/10.1029/2007GL030572

Wang, C., Chen, X., Zhao, K., & Peng, C.-H. (2024). Synoptic control on the initiation and rainfall characteristics of warm-season MCSs over the south China coast. *Journal of Geophysical Research: Atmospheres*, *129*(8), e2023JD039232. https://doi.org/10.1029/2023JD039232

Wang, J., Fan, J., & Feng, Z. (2023). Climatological occurrences of hail and tornadoes associated with mesoscale convective systems in the United States. *Natural Hazards and Earth System Sciences*, *23*(12), 3823–3838. https://doi.org/10.5194/nhess-23-3823-2023

Wang, X., Lu, H., & Yuan, W. (2022). Inter-annual variations of precipitation modulate the dry spell length. *GeoHealth*, *6*(4), e2022GH000611. https://doi.org/10.1029/2022GH000611

Weng, F., Han, Y., van Delst, P., Liu, Q., Kleespies, T., Yan, B., & Marshall, J. L. (2005). JCSDA community radiative transfer model (CRTM).

Yang, Q., Houze, R. A., Leung, L. R., & Feng, Z. (2017). Environments of long-lived mesoscale convective systems over the Central United States in convection permitting climate simulations. *Journal of Geophysical Research: Atmospheres*, *122*(24), 13288–13307. https://doi.org/10.1002/2017JD027033

Yang, R., Zhang, Y., Sun, J., Fu, S., & Li, J. (2019). The characteristics and classification of eastward-propagating mesoscale convective systems generated over the second-step terrain in the Yangtze River Valley. *Atmospheric Science Letters*, *20*(1), e874. https://doi.org/10.1002/asl.874

Zhan, Y., & Lin, Z. (2011). The relationship between June precipitation over mid-lower reaches of the Yangtze River basin and spring soil moisture over the East Asian monsoon region. *Acta Meteorologica Sinica*, *25*(3), 355–363. https://doi.org/10.1007/s13351-011-0310-6

Zhang, J., Guo, J., Li, J., Shao, J., Tong, B., & Zhang, S. (2022). The prestorm environment and prediction for local- and nonlocal-scale precipitation: Insights gained from high-resolution radiosonde measurements across China. *Journal of Geophysical Research: Atmospheres*, *127*(18), e2021JD036395. https://doi.org/10.1029/2021JD036395

Zhang, J., Wu, L., & Dong, W. (2011). Land-atmosphere coupling and summer climate variability over East Asia. *Journal of Geophysical Research*, *116*(D5), D05117. https://doi.org/10.1029/2010JD014714

Zhang, L. N., Gianotti, D. J. S., & Entekhabi, D. (2023). Land surface influence on convective available potential energy (CAPE) change during interstorms. *Journal of Hydrometeorology*, *24*(8), 1365–1376. https://doi.org/10.1175/JHM-D-22-0191.1

Zhao, M. (2022). A study of AR-TS-and MCS-associated precipitation and extreme precipitation in present and warmer climates. *Journal of Climate*, *35*(2), 479–497. https://doi.org/10.1175/JCLI-D-21-0145.1

Zhong, S., Yang, T., Qian, Y., Zhu, J., & Wu, F. (2018). Temporal and spatial variations of soil moisture – Precipitation feedback in East China during the East Asian summer monsoon period: A sensitivity study. *Atmospheric Research*, *213*, 163–172. https://doi.org/10.1016/j.atmosres.2018.05.014

Zhu, B., Xie, X., Meng, S., Lu, C., & Yao, Y. (2020). Sensitivity of soil moisture to precipitation and temperature over China: Present state and future projection. *Science of the Total Environment*, *705*, 135774. https://doi.org/10.1016/j.scitotenv.2019.135774

Zuo, Z., & Zhang, R. (2016). Influence of soil moisture in eastern China on the East Asian summer monsoon. *Advances in Atmospheric Sciences*, *33*(2), 151–163. https://doi.org/10.1007/s00376-015-5024-8